

Evaluation of metal artifacts in clinical MR images of patients with total hip arthroplasty using different metal artifact-reducing sequences

Gunilla M. Müller · Björn Lundin · Thord von Schewelov · Markus F. Müller · Olle Ekberg · Sven Månsson

Received: 26 May 2014 / Revised: 21 September 2014 / Accepted: 3 November 2014 / Published online: 5 December 2014
© ISS 2014

Abstract

Purpose To evaluate the distortion and artifact area of metal in MR images and to compare artifact reduction using different metal artifact-reducing sequences in patients with metal-on-metal (MoM) and non-MoM total hip prostheses.

Materials and methods Thirty-six MoM and 15 non-MoM prostheses were examined in a 1.5-T MR scanner using T1-weighted (T1-w) sequences: turbo spin echo (TSE) high-readout bandwidth (hiBW), T1-w; TSE view angle tilting (VAT), T1-w; TSE VAT+slice encoding for metal artifact correction (SEMAC); short tau inversion recovery (STIR) hiBW or matched RF pulses (mRFp). Distortion was quantified using a new method measuring the acetabular roof angle (ARA). The artifact area was defined in the mid-coronal plane of the artifact.

Results The T1 VAT+SEMAC sequence showed the least distortion compared to T1 VAT and T1-hiBW (150°, 127° and 102°, $p < 0.001$, in MoM; 152°, 143° and 128°, $p \leq 0.014$, in non-MoM). The artifact area was smaller in MoM prostheses using the T1 VAT sequence compared to T1 hiBW and T1 VAT+SEMAC (2506 mm², 3160 mm² and 3214 mm²,

$p < 0.001$) and smaller in non-MoM prostheses using T1 VAT compared to T1-hiBW (4296 mm² and 4831 mm², $p = 0.041$). STIR-mRFp substantially reduced the artifact size compared with STIR-hiBW (MoM 4559 mm² and 6323 mm²; non-MoM 5625 mm² and 8764 mm², $p < 0.001$).

Conclusion Metal artifacts in MR imaging examinations of hip prostheses can be evaluated for distortion using a distortion angle (ARA) and the degree of signal artifact as determined by measuring the largest cross-sectional artifact area. T1 VAT+SEMAC showed the least distortion; T1 VAT and STIR-mRFp were most efficient for reduction of the artifact area.

Keywords MR imaging · Metal artifact-reducing sequences (MARS) · Metal artifact · Hip · Hip prosthesis · Artifact measurement · Image distortion

Introduction

Magnetic resonance (MR) imaging is well suited to examine bone and soft tissue, but metal artifacts from prostheses hamper the visualization of periprosthetic tissues. The metal leads to variations in the static magnetic field, superimposing all imaging gradients and leads on the through-plane artifact (because of corruption of the slice selection gradient) as well as the in-plane artifact (because of corruption of the frequency encoding gradient). This results in a curved, thickened, thinned or split slice, seen as distortion, signal loss and pile-up effects in the MR image [1]. In inversion recovery sequences, severe artifacts can arise if the excitation and inversion slices are curved differently, since uninverted parts of the image will have different contrasts. The degree of artifacts in an image depends on the different components in the hip prosthesis as well as the different metal artifact-reducing

G. M. Müller (✉) · M. F. Müller · O. Ekberg
Department of Radiology, Lund University, Skåne University Hospital, Inga Marie Nilssonsgata 49, 20502 Malmö, Sweden
e-mail: gunilla.muller@med.lu.se

T. von Schewelov
Orthopedic Surgery, Lund University, Skåne University Hospital, Malmö, Sweden

S. Månsson
Medical Radiation Physics, Lund University, Skåne University Hospital, Malmö, Sweden

B. Lundin
Department of Radiology, Lund University, Skåne University Hospital, Lund, Sweden

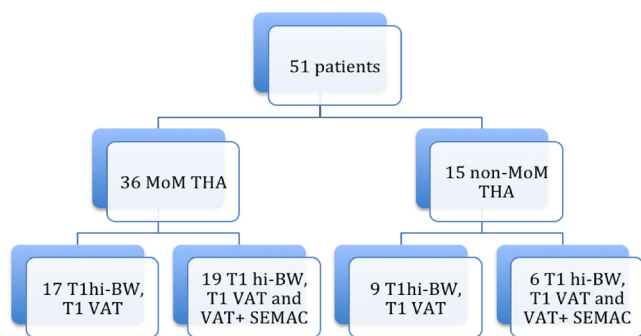


Fig. 1 Flowchart

sequence (MARS) methods applied [2]. Since metal-on-metal (MoM) prostheses have more metal components than non-MoM prostheses, the artifacts in the MR images are more severe with this first type.

Since the 1990s, the MR examination technique for patients with metallic implants has improved [3–6]. With high-bandwidth readout (hiBW), a reduction of the in-plane artifacts can be achieved. Further reduction of the in- and through-plane artifacts requires more in-depth changes of the imaging sequence. Cho et al. [7] used view angle tilting (VAT) to compensate for the distortion of the magnetic field. Later, VAT in combination with increased strength and higher bandwidth gradients was used in MARS [8]. Recently, a method called slice encoding for metal artifact correction (SEMAC), which corrects through-plane distortions by adding a phase-encoding gradient in the z-direction, was introduced [9]. Since SEMAC includes the VAT technique, it provides both in- and through-plane distortion corrections.

To optimize examinations of patients with hip prostheses, it is essential to be able to assess the extent of the metal artifacts in order to evaluate to what extent parts of

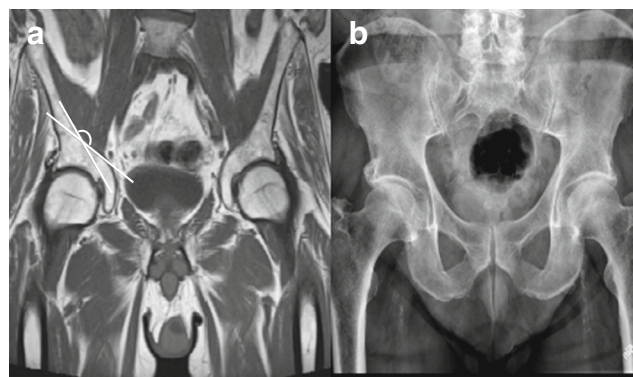


Fig. 2 Measurement of the normal acetabular roof angle (ARA) in a patient without THA in a central coronal slice of a T1-w image. TSE MR sequence (a) and conventional radiography (b)

bone or soft tissue are not visualized. To our knowledge, the extent of distortion in clinical images has not been measured previously. We observed that the shape of anatomic structures near a prosthesis changes with different MARS types and different hip prostheses. The angle formed by the legs of the inner margins of the os ilium and acetabular roof, the acetabular roof angle (ARA), is diminished with an increasing through-plane artifact in coronal slices near the center of the prosthesis, as the slices are bent in the examined volume. We hypothesize that the ARA can be used to measure the distortion (caused mainly by combined through- and in-plane artifacts). The measurement of signal loss and pile-up (in-plane artifacts) in the central slice based on the largest artifact area was introduced previously by Sutter et al. [10].

In this study, we apply the new ARA measure and the established artifact area quantification method in order to compare the distortion and artifact area caused by MoM and

Table 1 Sequence parameters

	T1-hiBW	T1 VAT	T1 VAT+SEMAC	STIR-hiBW	STIR-mRFp
Orientation	Coronal	Coronal	Coronal	Coronal	Coronal
Repetition time (ms)	480	492	480	4000	7150
Echo time (ms)	5	6	6	9	49
Inversion time (ms)				180	160
Echo train length	3	5	5	7	17
z-Encoding steps			12		
Frequency encoding	Head-foot	Head-foot	Head-Foot	Head-foot	Head-foot
Bandwidth (Hz/pixel)	751	977	977	395	685
Field of view (mm)	380×380	450×365	450×365	420×420	420×420
Matrix	512×384	512×312	512×312	384×288	384×288
Slice thickness (mm)	3	2.5	4	3	3
Scan time (min)	6:11	6:15	6:34	2:54	4:12

Table 2 Acetabular roof angle (ARA) angle in ten patients without metal implants in the T1-w sequence (7 males, 3 females)

	Angle right (°)	Angle left (°)	Age (years)
Mean	163	164	49
Median	162	164	53
Min	151	156	20
Max	180	173	73

non-MoM total hip prostheses when using different MARSs: T1-hiBW, T1 VAT and T1 VAT+SEMAC as well as STIR-hiBW and STIR with matched RF pulses (mRFp).

Materials and methods

Patients

The hospital's Ethics Committee approved the study, and all participants gave their written consent.

Measurements were conducted in 36 patients with MoM THA (13 males, 23 females; mean age 57, range 33–72 years) and 15 patients with non-MoM THA (6 males, 9 females; mean age 65, range 40–82 years) as described in the flowchart (Fig. 1). All recruited patients in both groups were routine clinical cases. Exclusion criteria were standard contraindications for MR investigation.

In the group with MoM prostheses, T1-hiBW and T1 VAT sequences were applied in 17 and T1-hiBW, T1 VAT and T1 VAT+SEMAC in 19 patients. In the non-MoM prosthesis group, T1-hiBW and T1 VAT sequences were applied in nine and T1-hiBW, T1 VAT and T1 VAT+SEMAC in six patients. Fewer patients were investigated with SEMAC because this sequence was not available at the time the first patients were examined.

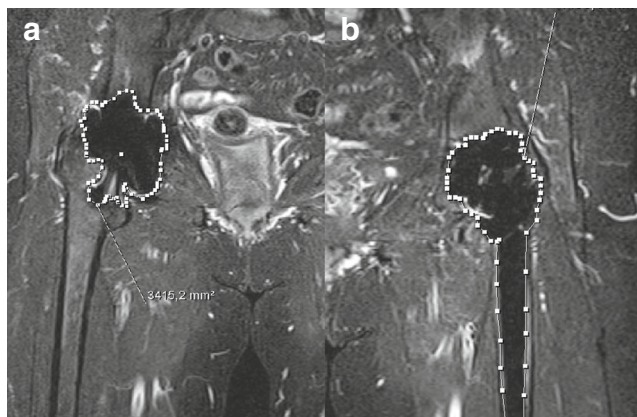


Fig. 3 The largest artifact area outlined in a STIR mRFp central coronal slice of a MoM prosthesis (a) and in the region of the stem in a prosthesis with stainless steel (b)

The STIR-hiBW and STIR-mRFp sequences were applied in the first 14 and 8 patients with MoM and non-MoM prostheses, respectively, but thereafter only the STIR-mRFp was applied since the artifact size was indisputably better reduced using this latter sequence.

MR imaging

Imaging was conducted with a 1.5-T MRI system (MAGNETOM Avanto; Siemens AG, Healthcare Sector, Erlangen, Germany) using the spine matrix and body matrix coils. The imaging protocol (Table 1) comprised three T1-weighted (T1-w) sequences: TSE with a high-readout bandwidth (T1-hiBW), TSE with VAT (T1 VAT), and TSE with both VAT and SEMAC (T1 VAT+SEMAC) and two inversion recovery sequences: one with a high-readout bandwidth (STIR-hiBW) and one with matched RF pulses (STIR-mRFp). The parameters of the T1 VAT+SEMAC were set to equal the scan time of the T1 VAT sequence. In the STIR-mRFp sequence, equal curving of the excitation and inversion slices near the prosthesis was obtained by matching the bandwidths of the excitation and inversion RF pulses, i.e., the same slice gradient strength was used for both pulses. T1 VAT, T1 VAT+SEMAC and STIR-mRFp were prototype sequences ('WARP' works-in-progress sequence package, Siemens AG).

Measurement of the distortion and artifact area

The angle formed by the legs of the inner margins of the os ilium and the acetabular roof in the coronal center slice of the hip, the acetabular roof angle (ARA), was used to measure the distortion (Fig. 2). Measurement of the right and left hip in MR examinations of ten patients without THA showed an $ARA > 150^\circ$ (Table 2). The artifact area was measured by visual outlining of the artifact (defined as the area with signal void and pile-up artifacts, i.e., low and high signal) in the location of the prosthesis and surroundings (Fig. 3). The artifact area was delineated in the central slice through the prosthesis with the largest area as described by Sutter et al. [10]. The examinations were reviewed by two experienced musculoskeletal radiologists, BL with >25 years and GM with 8 years of musculoskeletal radiology experience.

Statistical analysis

Statistical analyses were performed with statistical software (IBM SPSS Statistics, release 21.0, Chicago, IL). Descriptive statistics were used to calculate the mean and range of the distortion angle and the artifact area. A paired *t*-test was applied to evaluate the ARA and artifact areas using the different sequences. The distortion angle was compared between the MoM and non-MoM prosthesis groups using the

Fig. 4 The ARA is small in T1-hiBW (a+d), less reduced in T1 VAT (b+e) and normal in T1 VAT+SEMAC (c+f)

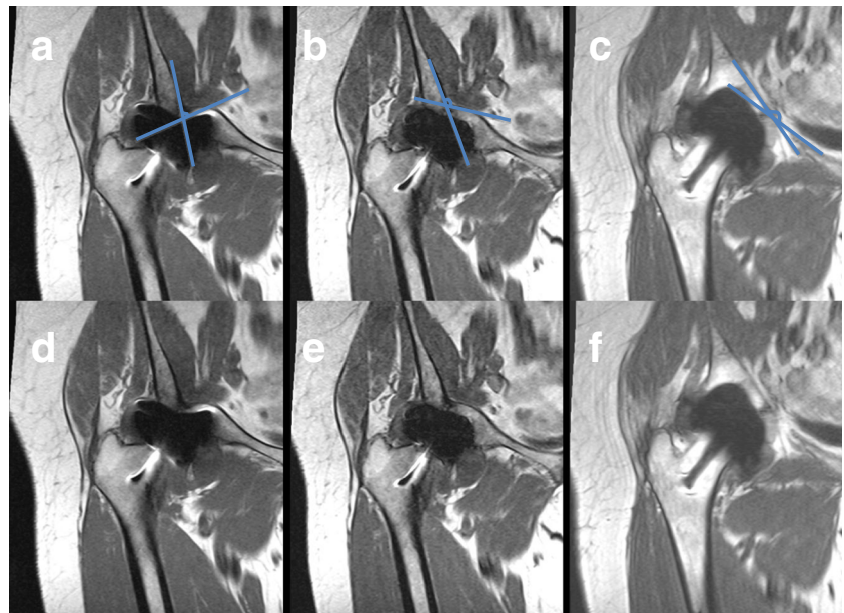


Table 3 Descriptive statistics of the distortion angle ARA

	T1-hiBW	T1 VAT	T1 VAT+SEMAC	STIR-hiBW	STIR-mRFp
	Mean (°)	Mean (°)	Mean (°)	Mean (°)	Mean (°)
	Range (°)	Range (°)	Range (°)	Range (°)	Range (°)
	n =	n =	n =	n =	n =
MoM prosthesis	102	127	150	Not measurable	96
	70–139	85–157	116–180		75–109
	36	36	19		14
Non-MoM prosthesis	128	143	152	Not measurable	121
	104–147	117–162	146–171		103–143
	15	15	6		15

Fig. 5 Coronal image of an MoM prosthesis with different T1-w. sequences; T1-hiBW (a) shows large metal artifacts, T1 VAT (b) with a reduced artifact area and T1 VAT+SEMAC (c) with no distortion

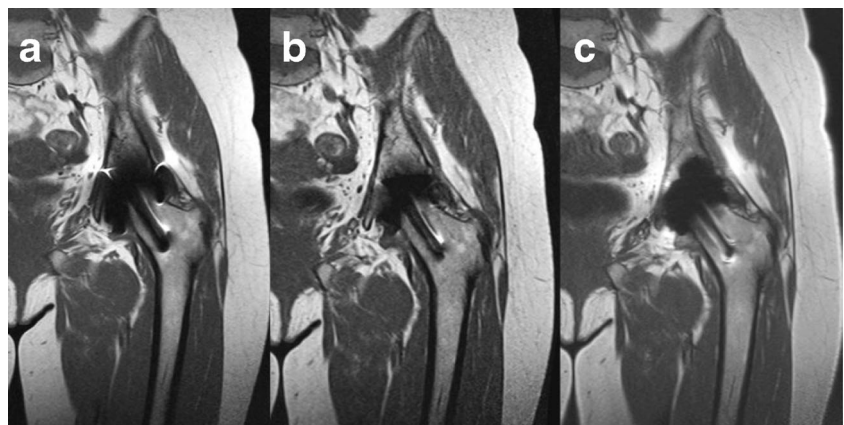


Table 4 Wilcoxon-Mann-Whitney test of the difference between the angles of MoM and non-MoM prostheses in the different sequences. The iliopectineal angle could not be measured in STIR-hiBW because of the large artifact size

Sequence	T1-hiBW	T1 VAT	T1 VAT+SEMAC	STIR-mRFp
U	31.500	79.000	45.500	12.500
Z	-4.108	-2.855	-0.143	-3.930
p	0.000	0.004	0.887	0.000

Wilcoxon-Mann-Whitney test. The artifact areas could not be compared between the groups of MoM and non-MoM prostheses since the prostheses differed in size. The level for statistical significance was $p \leq 0.05$.

Results

Analysis of the distortion and artifact area

The ARA varied with the different MARS sequences (Fig. 4). The angle was smaller than normal in T1-hiBW and STIR-mRFp in all prostheses and in the VAT in the MoM prostheses. The T1 VAT+SEMAC showed a normal angle in MoM as well as non-MoM prostheses. The statistics of the measured angles are listed in Table 3. Comparing the different prostheses, the ARA was smaller in the MoM compared to the non-MoM prostheses, i.e., showed more distortion in the first type. In both MoM and non-MoM prostheses, the *t*-test showed significantly less distortion in T1 VAT+SEMAC than T1-hiBW ($p < 0.001$ and $= 0.006$, respectively), in T1 VAT+SEMAC than T1 VAT ($p < 0.001$ and $= 0.014$) and in T1

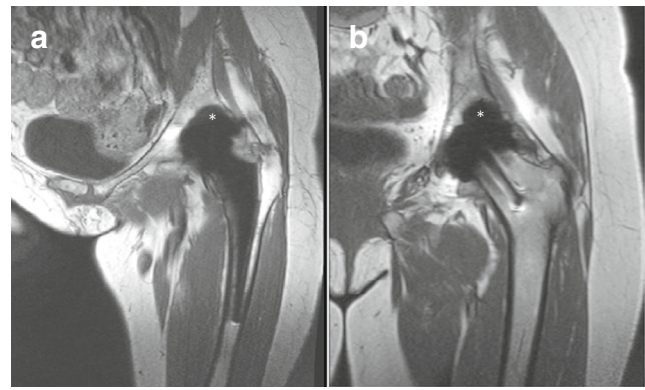


Fig. 7 T1 VAT+SEMAC sequence (a) with a characteristic large artifact subsequent to the prosthesis cup (*) in a non-MoM prosthesis with a titanium cup and long titanium steel and (b) in surface replacement

VAT than T1-hiBW ($p < 0.001$) (Fig. 5). Comparing the distortion between MoM and non-MoM prostheses, the Wilcoxon-Mann-Whitney test revealed significantly more distortion in MoM prostheses (Table 4). The ARA could not be measured in STIR-hiBW because of the large artifact size.

The artifact area varied with the different types of prostheses as well as the material of the prosthesis components (Figs. 5 and 6). In the MoM prosthesis, the artifact area in the T1 VAT+SEMAC sequence was similar to that in the T1-hiBW sequence. Despite the better delineation of the MoM implant with SEMAC, it does, however, show an additional area of signal void adjacent to the cranial aspect of the acetabular component (Fig. 7), which is why the total artifact area is not improved compared to the VAT sequence without SEMAC. The STIR-mRFp showed significantly less artifact area compared to the STIR-hiBW (Fig. 8). The descriptive statistics of the artifact area are listed in Table 5.

In the patients with MoM prostheses, the *t*-test showed a significantly smaller artifact area in the T1 VAT compared to

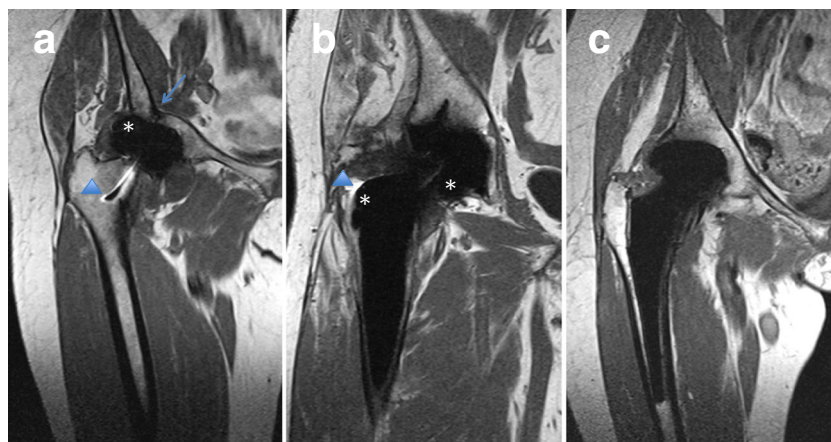


Fig. 6 Artifacts in the T1 VAT images of (a) an MoM prosthesis with large artifacts in the cup region with low signal (*) and pile-up effect (arrowhead) in the femoral region and distortion (arrow), (b) a prosthesis with a cemented metal cup with a polyethylene lining and cemented

stainless steel stem with a large artifact in the cup and stem region but less distortion since the lining is not metal and (c) a prosthesis with a cemented cup with non-MoM and uncemented titanium steel showing fewer artifacts in the cup and stem region

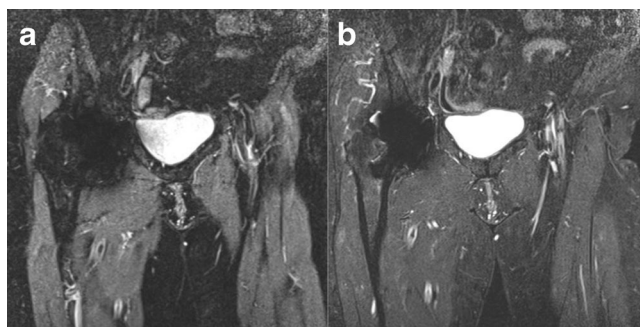


Fig. 8 Coronal images of an MoM prosthesis; STIR-hiBW showing large artifacts (a) and STIR-mRFp with reduced artifacts (b)

T1-hiBW ($p=0.00$, $n=36$) and to the T1 VAT+SEMAC sequence ($p=0.00$, $n=19$), but no difference in artifact size between the T1-hiBW and T1 VAT+SEMAC sequence ($p=0.93$, $n=19$). In the patients with non-MoM prostheses, a significant difference was revealed between the T1 VAT and T1-hiBW sequence ($p=0.041$, $n=15$), but no difference between the T1 VAT and T1 VAT+SEMAC sequence ($p=0.18$, $n=6$) or between the T1-hiBW and T1 VAT+SEMAC sequence ($p=0.41$, $n=6$) was revealed.

The t -test showed a significant difference in the artifact area between the STIR-mRFp and STIR-hiBW in patients with MoM prostheses ($p<0.001$, $n=14$) and non-MoM prostheses ($p<0.001$, $n=8$) with smaller artifacts in the STIR-mRFp.

Discussion

The variation in the magnetic field around metal prostheses results in the in- and through-plane distortion of the image [1], seen as a deformation of the anatomic shape of the surrounding tissues. This is particularly the case for the bone near the prostheses; therefore, the angle formed by the legs of the inner margins of the os ilium and acetabular roof in the coronal center slice of the hip, the acetabular roof angle (ARA), is well suited to measure the distortion. The ARA will diminish with increasing distortion and is therefore reciprocal to the distortion. To our knowledge, a measurement of image distortion in

clinical MR examinations of hip prostheses has not been previously reported.

Regarding the artifacts in the prostheses groups in our study, there was more distortion in the MoM prosthesis group, but artifact areas were overall larger in the non-MoM prosthesis group, with wide ranges of the measurement of distortion and artifact area in both groups. These variations were caused by the difference in material in the prosthesis components between and within the groups. The acetabular component of the MoM prostheses consisted of a cobalt-chromium alloy and of the non-MoM of a polyethylene liner. The stem in MoM prostheses varied from a short cobalt-chromium alloy base in the surface replacements to a long titanium stem in non-surface replacement prostheses. In the non-MoM prosthesis, the stem was of stainless steel or titanium. Since we compared the sequences in the same patients, the differences of the prosthesis parts did not affect the results.

Our results are similar to those of a recent study by Sutter et al. [10] regarding the small artifact area using a modified STIR sequence optimized for metal artifact reduction, but differ from this study as we found a smaller artifact area also in T1 VAT compared to the T1-hiBW and T1 VAT+SEMAC. These authors did not specify the type of prosthesis in their study. However, we think the different experiences regarding the latter type of sequence could be due to different cup materials in the studies, with more MoM prostheses in our material.

As expected, there was less distortion on average when imaging any type of prosthesis using both the in- and through-plane correcting T1 VAT+SEMAC sequence. In the non-MoM prostheses, the distortion in T1 VAT was also low but still higher compared with T1 VAT+SEMAC. The T1 VAT showed a significantly smaller artifact area than T1-hiBW in MoM and non-MoM prostheses as well as T1 VAT+SEMAC in MoM prostheses. The latter result of an increased artifact area with SEMAC may seem surprising; however, this is a consequence of a wrap-around artifact in the slice selection direction due to a trade-off in scan time, making the number of z -encoding steps in T1 VAT+SEMAC insufficient for a full correction of the curved slice.

Table 5 Descriptive statistics of the artifact area

	T1-hiBW	T1 VAT	T1 VAT+SEMAC	STIR-hiBW	STIR-mRFp
	Mean (mm ²)	Mean (mm ²)	Mean (mm ²)	Mean (mm ²)	Mean (mm ²)
	Range (mm ²)	Range (mm ²)	Range (mm ²)	Range (mm ²)	Range (mm ²)
	n =	n =	n =	n =	n =
MoM prosthesis	3160	2506	3214	6323	4559
	1804–7179	1308–5924	2010–6777	4391–9406	2753–8671
	36	36	19	14	36
Non-MoM prosthesis	4831	4296	4805	8764	5625
	3028–7396	1178–7242	3096–6709	6029–11,290	3148–8465
	15	15	6	8	15

Consequently, a limitation of our study is that the T1 VAT+SEMAC was designed to have a similar scan time as the other T1-weighted sequences. The scan time for each sequence was slightly more than 6 min; if further increased, the additional motion artifacts would be a potential drawback. The scan time in T1 VAT+SEMAC increases proportionally to the number of *z*-encoding steps, and the time restraint restricted the number of such steps to 12, which in some cases was not sufficient to restore the curved slice and resulted in severe signal voids due to artifact folding in the *z*-direction (slice selection direction); a further optimized sequence would require about 16 min. Thus, in this specific context the artifact area measure was influenced not only by an in-plane but also a through-plane effect. In the future, if further technical improvements reduce the acquisition time of the T1 VAT+SEMAC sequence and allow more *z*-encoding steps to be applied, this sequence may provide an overall superior performance in artifact reduction.

In summary, the new measure ARA can be used to evaluate metal-induced image distortion. Applying ARA as well as a previously described artifact area quantification method, we found the metal artifacts significantly reduced in MARS T1 VAT+SEMAC, T1 VAT and STIR-mRFP compared to MARS with only high bandwidth in both MoM and non-MoM prostheses.

Conflicts of interest None of the authors has a financial interest.

References

1. Hargreaves BA, Worters PW, Pauly KB, Pauly JM, Koch KM, Gold GE. Metal-induced artifacts in MRI. *AJR Am J Roentgenol*. 2011;197:547–55.
2. Lee MJ, Kim S, Lee SA, et al. Overcoming artifacts from metallic orthopedic implants at high-field-strength MR imaging and multi-detector CT. *Radiographics*. 2007;27:791–803.
3. Lee MJ, Janzen DL, Munk PL, MacKay A, Xiang QS, McGowen A. Quantitative assessment of an MR technique for reducing metal artifact: application to spin-echo imaging in a phantom. *Skeletal Radiol*. 2001;30:398–401.
4. Potter HG, Nestor BJ, Sofka CM, Ho ST, Peters LE, Salvati EA. Magnetic resonance imaging after total hip arthroplasty: evaluation of periprosthetic soft tissue. *J Bone Joint Surg Am*. 2004;86-A:1947–54.
5. Suh JS, Jeong EK, Shin KH, et al. Minimizing artifacts caused by metallic implants at MR imaging: experimental and clinical studies. *AJR Am J Roentgenol*. 1998;171:1207–13.
6. White LM, Kim JK, Mehta M, et al. Complications of total hip arthroplasty: MR imaging-initial experience. *Radiology*. 2000;215:254–62.
7. Cho ZH, Kim DJ, Kim YK. Total inhomogeneity correction including chemical shifts and susceptibility by view angle tilting. *Med Phys*. 1988;15:7–11.
8. Olsen RV, Munk PL, Lee MJ, et al. Metal artifact reduction sequence: early clinical applications. *Radiographics*. 2000;20:699–712.
9. Lu W, Pauly KB, Gold GE, Pauly JM, Hargreaves BA. SEMAC: slice encoding for metal artifact correction in MRI. *Magn Reson Med*. 2009;62:66–76.
10. Sutter R, Ulbrich EJ, Jellus V, Nittka M, Pfirrmann CW. Reduction of metal artifacts in patients with total hip arthroplasty with slice-encoding metal artifact correction and view-angle tilting MR imaging. *Radiology*. 2012;265:204–14.